PHOTOELECTRIC AND THERMIONIC PROPERTIES OF NICKEL

by

HELEN ISABEL PETERSON

B. S., Kansas State College
of Agriculture and Applied Science, 1940

A THESIS

submitted in partial fulfillment of the

requirements for the degree of

MASTER OF SCIENCE

Department of Physics

KANSAS STATE COLLEGE
OF AGRICULTURE AND APPLIED SCIENCE

1943

TABLE OF CONTENTS

INTRODUCTION

The discovery of the surface photoelectric effect was made by Hertz (33) in 1887. During the course of experiments utilizing spark gaps, Hertz discovered that if light shone on the electrodes the arc would start more easily. It was shown in later experiments by Hallwachs (32) that the light caused emission of electrons from the negative terminal. This electron emission due to electromagnetic radiation is called the photoelectric effect.

This phenomenon has been of great importance in the development of modern physics. Not long after the photoelectric effect was discovered, Lenard (39, 40) showed that some of its most important aspects could not be interpreted in terms of the wave theory of light. In 1905, Einstein (22, 23) applied the quantum theory to photoelectricity, resulting in his famous equation,

$$E = 1/2\ mv^2 = h\nu - \phi$$

where E = kinetic energy of emitted electron,

m = mass of electron,

v = velocity of electron in centimeters per second,

h = Planck's constant,

ν = frequency of the radiation falling on the surface,

and ϕ = work function of emitting surface in ergs (energy required to remove an electron from the substance).

Einstein's equation supplied a direct connection between the photoelectric effect and the quantum theory of radiation.

His equation was later experimentally verified by Hughes (35), Richardson and Compton (50), and Millikan (45).

Recently it has been found that photoelectrons released from metals are capable not only of yielding information about the nature of the radiation which freed them, but also about the metal from which they escaped. Thus the field of photoelectricity is closely bound up with the new electron theory of metals and also the new quantum theory.

The basis for the new electron theory of metals was established in 1928 by Sommerfeld (51). Prior to that time electrical phenomena were interpreted in terms of the classical electron-gas theory developed by Drude, Lorentz, and others. Although the classical theory was successful in some respects and did not conflict directly with any of the known facts in the field of photoelectricity, it offered no explanation of the energy distribution of photoelectrons and the variation of photocurrent with frequency--two of the fundamental problems in this field. This theory postulated an average thermal energy of the electrons which was so small (about 0.04 electron-volt at 300°K) that it could be neglected in comparison with the energy of an average impinging quantum (4 to 6 electron-volts). Neglecting this thermal energy the Einstein theory led at once to two important conclusions:

1. There is a sharply defined maximum velocity v_m of emission of photoelectrons which is related to the frequency by the equation, $1/2\ mv_m^2 = h\nu - \phi = h\nu - h\nu_o$

2. There is a sharply defined threshold frequency ν_o such that incident light of frequency less than this, no matter how intense, will not produce a photoelectric emission.

The classical theory assumes that the energies of the "free" electrons in metals are distributed according to the Maxwellian distribution function, while the Sommerfeld theory treats the electrons as a degenerate gas obeying the Fermi-Dirac statistics. In 1931, with the Sommerfeld theory as a basis, Fowler (28) developed a theory of spectral distribution as applied to photoelectrons which has proved quite successful in determining the important characteristics of metal surfaces from experimental data. This theory emphasizes that the above conclusions with regard to Einstein's theory are accurately true only for a metal surface at the temperature 0°K while at higher temperatures there will not be a sharply defined maximum velocity or threshold frequency. It predicts the actual form of the energy distribution and spectral distribution curves at any temperature and presents a method of determining the value of v_m and ν_o which the surface would show at 0°K if the lowering of the temperature produced no other changes in the character of the surface. The theoretical curve obtained by Fowler is shown in Fig. 1. Experimental data for any metal can be fitted to this curve, thereby enabling one to determine the work function.

It is evident from Sommerfeld's theory that the photoelectric work function of a metal determined by Fowler's method should be the same as the thermionic work function in

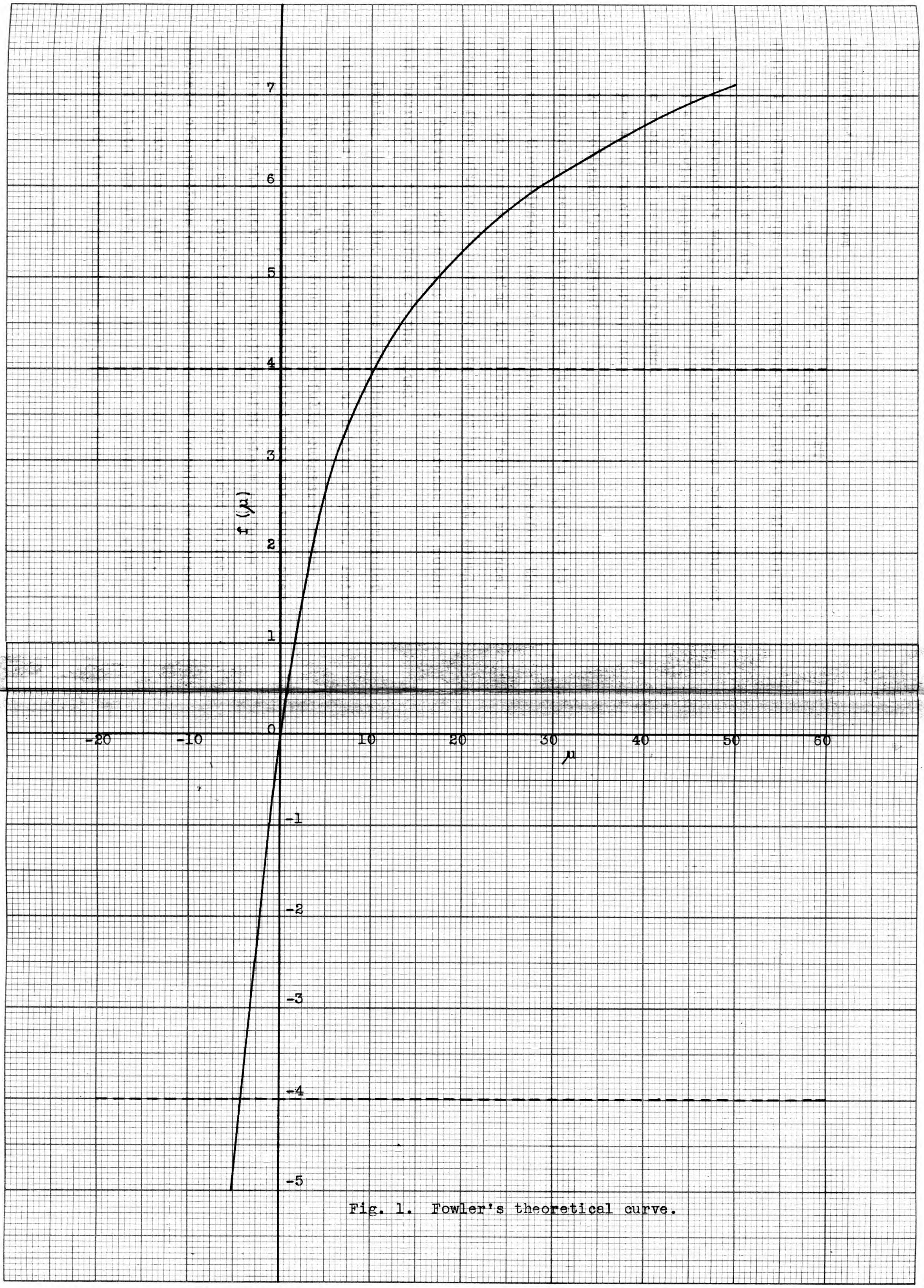

Fig. 1. Fowler's theoretical curve.

Richardson's well-known equation,

$$I = AT^2 e^{-b/T} = AT^2 e^{-\phi/kT}$$

where I = emission current in amperes per square centimeter of emission surface,

A and b = parameters which depend on the surface being studied,

T = Kelvin temperature,

e = base of natural logarithms,

ϕ = work function in ergs, and

k = Boltzmann's constant.

This conclusion seems reasonable as Richardson's equation is based upon thermodynamic considerations alone. Therefore the origin of the energy releasing the electron from the surface, whether from within the metal or outside of the metal, should not be a factor in the energy necessary to overcome the potential barrier at the surface of the metal.

During the last two decades experimenters have perfected photoelectric and thermionic technique to a high degree. Prior to this, no work had been done on carefully outgassed metal surfaces in high vacuum, and data obtained were not truly characteristic of the metal. When working with clean surfaces in a high vacuum, stable conditions have been reached and reliably accurate observations of photoelectric and thermionic characteristics have been made on a number of different elements. Table 1 lists the metals which have been studied along with the names of the experimenters who did the work.

Table 1. Metals which have been studied for their photoelectric and thermionic properties since 1925.

Metal	Experimenter
Barium	Jamison and Cashman (36)
	Cashman and Bassoe (10)
Bismuth	Jupnik (37)
Cadmium	Bomke (2)
Calcium	Jamison and Cashman (36)
Carbon	Reiman (49)
Cobalt	Cardwell (5, 6)
Columbium	Wahlin and Sordahl (55)
Gold	Morris (46)
Iron	Cardwell (7)
Mercury	Kazda (38)
	Dunn (21)
	Hales (31)
Magnesium	Cashman and Huxford (11, 12)
Molybdenum	Martin (41)
	DuBridge and Roehr (19)
	Wahlin and Reynolds (54)
	Wright (63)
Palladium	DuBridge and Roehr
Platinum	DuBridge (17, 18)
	Whitney (60)
Rhenium	Engelmann (24)
Rhodium	Dixon (16)
Silver	Winch (61)
	Winch and Farnsworth (62)
Tantalum	Cardwell (8, 9)
Tin	Goetz (30)
Tungsten	Warner (57, 58, 59)
Uranium	Hole and Wright (34)
Zinc	Dillon (15)
	DeVoe (14)

Lattice spacing and crystal structure as well as traces of gas on the surface of metals have been found to affect markedly the work function of metals and also other physical properties. A change in the crystal structure and lattice spacing was observed to cause a variation in the photoelectric and thermionic work functions of iron (7) and cobalt (5, 6) and in the photoelectric work function of tin (30), and practically every worker in the field has recorded tremendous shifts in the work function as the occluded gas in the metal is removed in high vacuum. It is, therefore, of interest to study other metals photoelectrically, and in this work nickel was selected.

Investigators of the physical properties of nickel are unable to agree entirely on the nature of the crystallographic change which may occur in nickel between 300 and 400°C. Merica (44) has reported a change in the specific heat and specific resistance of nickel in this temperature interval. Work on other metals by Masumoto (42) indicates that such changes are usually associated with a crystal transformation. Ewert (25) has concluded that although the data about the allotropism of nickel are still confusing, there exists a cubic face-centered α-form stable at ordinary temperatures exactly as in the case of iron and cobalt, and that the change of α-nickel at about 350°C from the ferromagnetic into the feebly paramagnetic β-state is not accompanied by a crystallographic change. However, between these two states, he believes there exists for a

very short temperature interval a hexagonal close-packed structure. In 1927, Bredig and Allolio (3) announced their discovery of the hexagonal close-packed nickel. In 1929, Mazza and Nasini (43) concluded from their experiments that nickel obtained by three different methods crystallized in face-centered cubes and that pure cold-drawn nickel after various thermal treatments, although sometimes showing peculiar re-crystallization, always crystallized in face-centered cubes. Later that year Thompson (52), by means of electron diffraction, presented data for the existence of the hexagonal form of nickel. He believed, however, because of the low density of the sample obtained by Bredig and Allolio, that they had studied a hydride of nickel rather than the pure metal. Bredig and Schwarz von Bergkampf (4) then prepared nickel samples by two different methods and again obtained data indicating the existence of hexagonal close-packed nickel.

It was felt that a study of the photoelectric and thermionic emission of a clean nickel surface at various temperatures might present more definite evidence concerning these crystallographic transformations as well as information about the photoelectric and thermionic properties of nickel.

EXPERIMENTAL APPARATUS AND PROCEDURE

The apparatus consisted essentially of a strip of nickel suspended in a specially constructed tube connected to a vacuum system. Ultraviolet light falling on the nickel was

made monochromatic by means of a Bausch and Lomb monochromator. The very small electron currents were measured by a specially designed amplifying tube and circuit.

The general arrangement of the apparatus is shown in Plate I. The experimental tube is approximately in the center of the photograph enclosed in a large sheet iron box to eliminate stray induced currents. Just above the tube is the ionization gauge used to determine pressures. The gauge and the tube are connected through a liquid air trap and a mercury cut-off to a single-stage, water-cooled mercury vapor pump backed by a Welch Duo-seal vacuum pump. To the right of the tube a part of the Bausch and Lomb monochromator can be seen. The quartz mercury arc is behind the three galvanometers. On the table in the fore part of the picture are parts of the ionization gauge circuit and of the electrometer circuit, the instrument panel of the electrometer circuit being on the far right.

The Experimental Tube

A detailed diagram of the experimental tube is given in Plate II. The strip to be tested consisted of a ribbon of nickel, 0.03 mm thick, 4 mm wide, and 12 cm long, suspended by Kovar-tungsten leads in the form of a loop. The sample was electrolytic spectroscopically pure nickel, obtained from Adam Hilger, London.

Radiation from the quartz mercury arc could be focused onto the nickel through a quartz window sealed directly to

EXPLANATION OF PLATE I

Photograph of the apparatus.

PLATE I

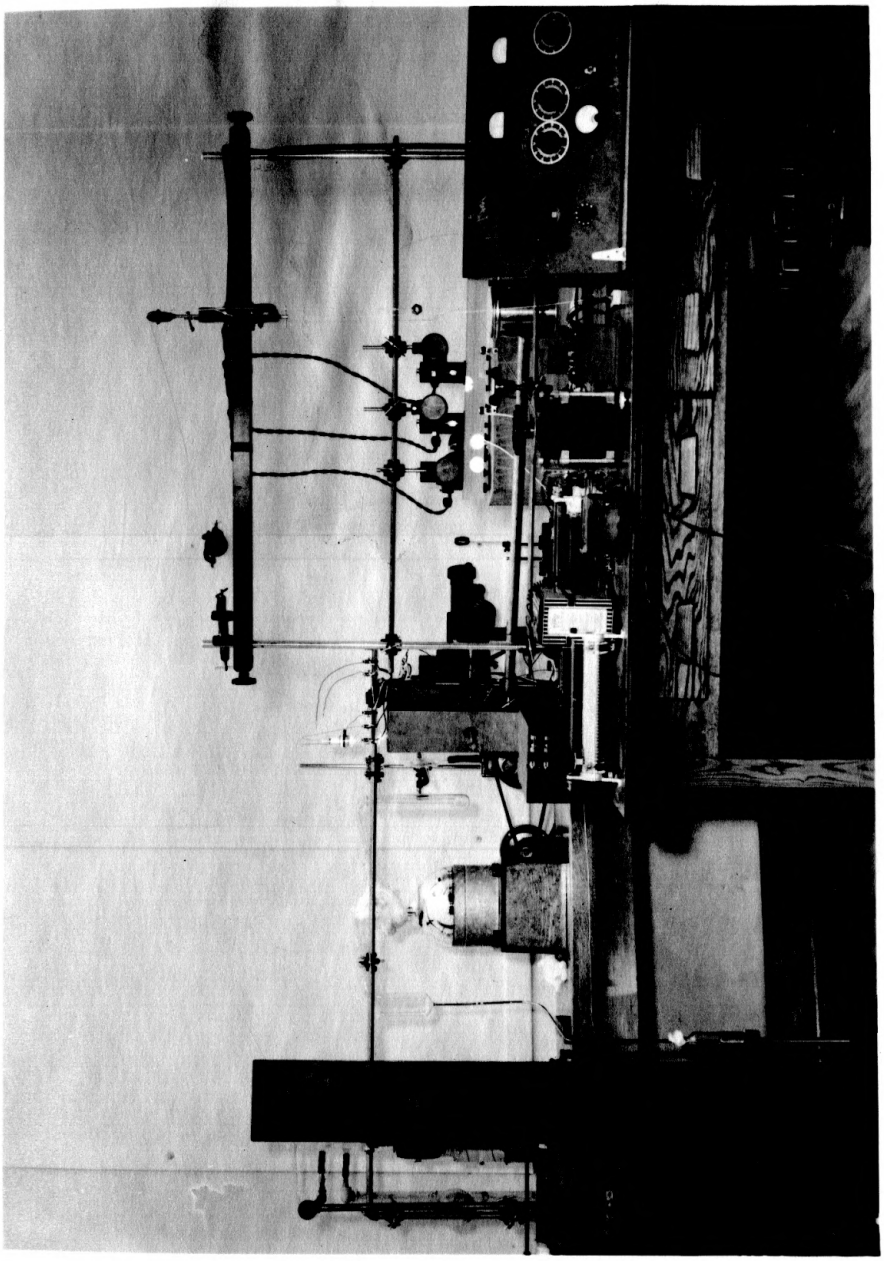

EXPLANATION OF PLATE II

Diagram of the experimental tube.

PLATE II

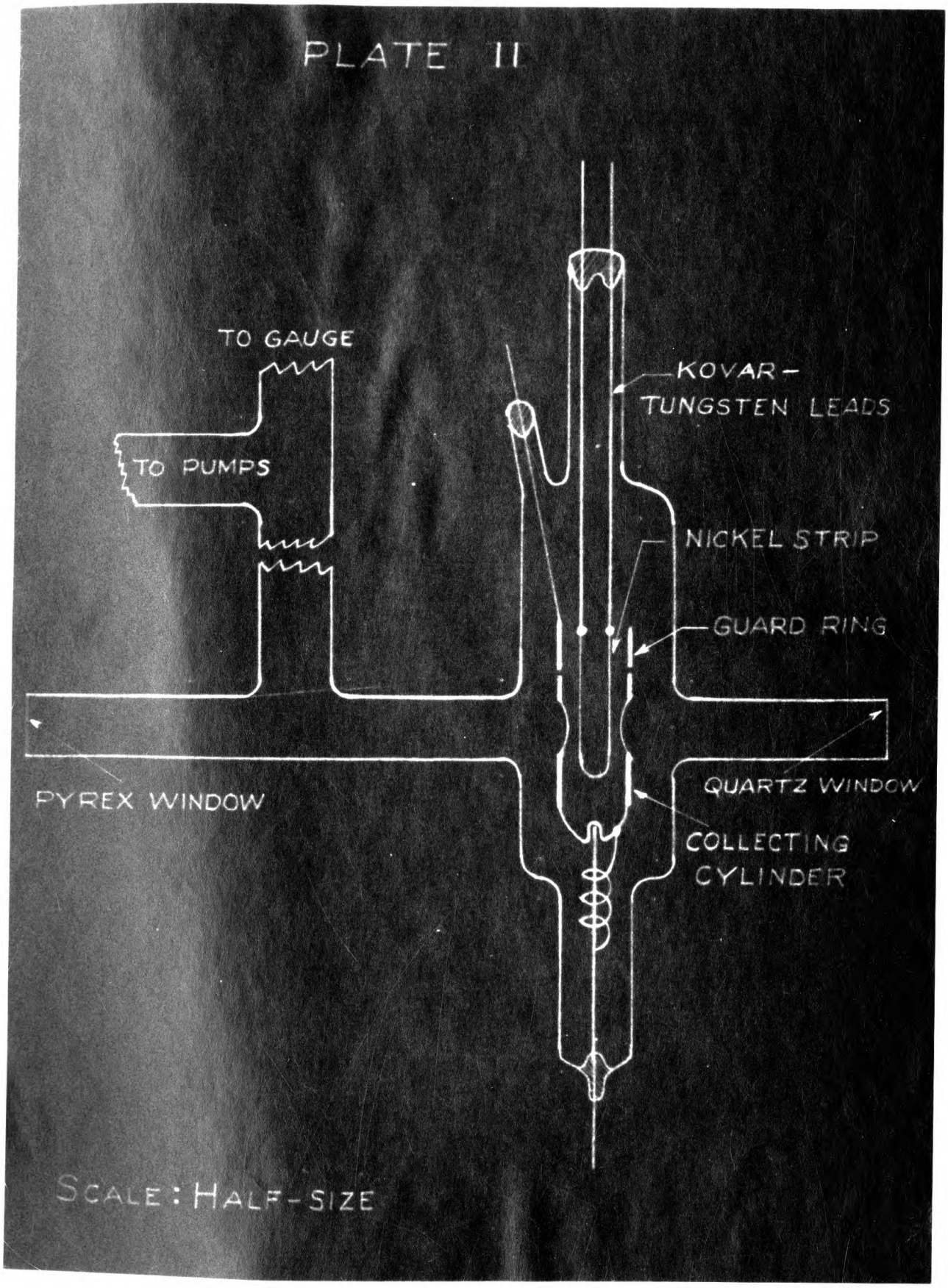

SCALE: HALF-SIZE

the pyrex tube by means of a graded joint. An optically flat pyrex window was provided on the opposite side of the tube for making temperature observations. Just opposite these windows were openings in the molybdenum collecting cylinder. While heating the sample at high temperatures, the cylinder was turned by means of an external magnet to prevent the distillation of nickel onto the quartz window and the pyrex window. A guard ring was placed above the collecting cylinder so that only electrons emitted from the lower portion of the loop were collected by the cylinder.

The Electrometer Circuit

The electron currents to be measured were of the order of 10^{-15} amp. Therefore, a very sensitive current-registering device was needed. A Compton quadrant electrometer (13) was used in a number of the earlier experiments of this type. In recent years experimenters have been using vacuum tubes with a high input resistance designed especially to amplify extremely small currents. The Western Electric D-96475 tube was used in this experiment; the General Electric FP-54 is also designed for this type of work.

The circuit used for the D-96475 tube is shown in Plate III, along with a schematic representation of the experimental tube and its electrical connections. This electrometer tube circuit is essentially the one developed by Barth (1). In a circuit of this type, stability is of utmost importance; but

EXPLANATION OF PLATE III

The electrometer circuit, showing connections to the experimental tube.

A - Experimental tube.

B - Western Electric No. D-96475 tube.

G - Leeds and Northrup galvanometer, sensitivity 0.0001 μa/mm, damping resistance 18,000 ohms, internal resistance 539 ohms, period 14.1 sec.

K_1 - High insulation key.

K_2 - DPDT switch.

K_3 - SPDT switch.

I_s - Weston A.C. ammeter, range 0-25 amp.

I_p - Triplett D.C. microammeter, range 0 to 100 μa.

I_n - Triplett D.C. milliammeter, range 0-1 ma.

I_f - Weston D.C. milliammeter, range 0-300 ma.

R_g - 1.06×10^{10} ohms fixed resistance.

R_p - 0 to 100,000 ohms adjustable resistance.

R_n - 0 to 100,000 ohms adjustable resistance.

R_b - 0 to 7 ohms adjustable resistance.

R_f - 0 to 7 ohms adjustable resistance.

R_1 - 11.1 ohms fixed resistance.

R_2 - 13 ohms fixed resistance.

R_3 - 6 ohms fixed resistance.

R_4 - 18,000 ohms fixed resistance.

R_5 - 523 ohms fixed resistance.

R_6 - 1046 ohms fixed resistance.

R_7 - 523 ohms fixed resistance.

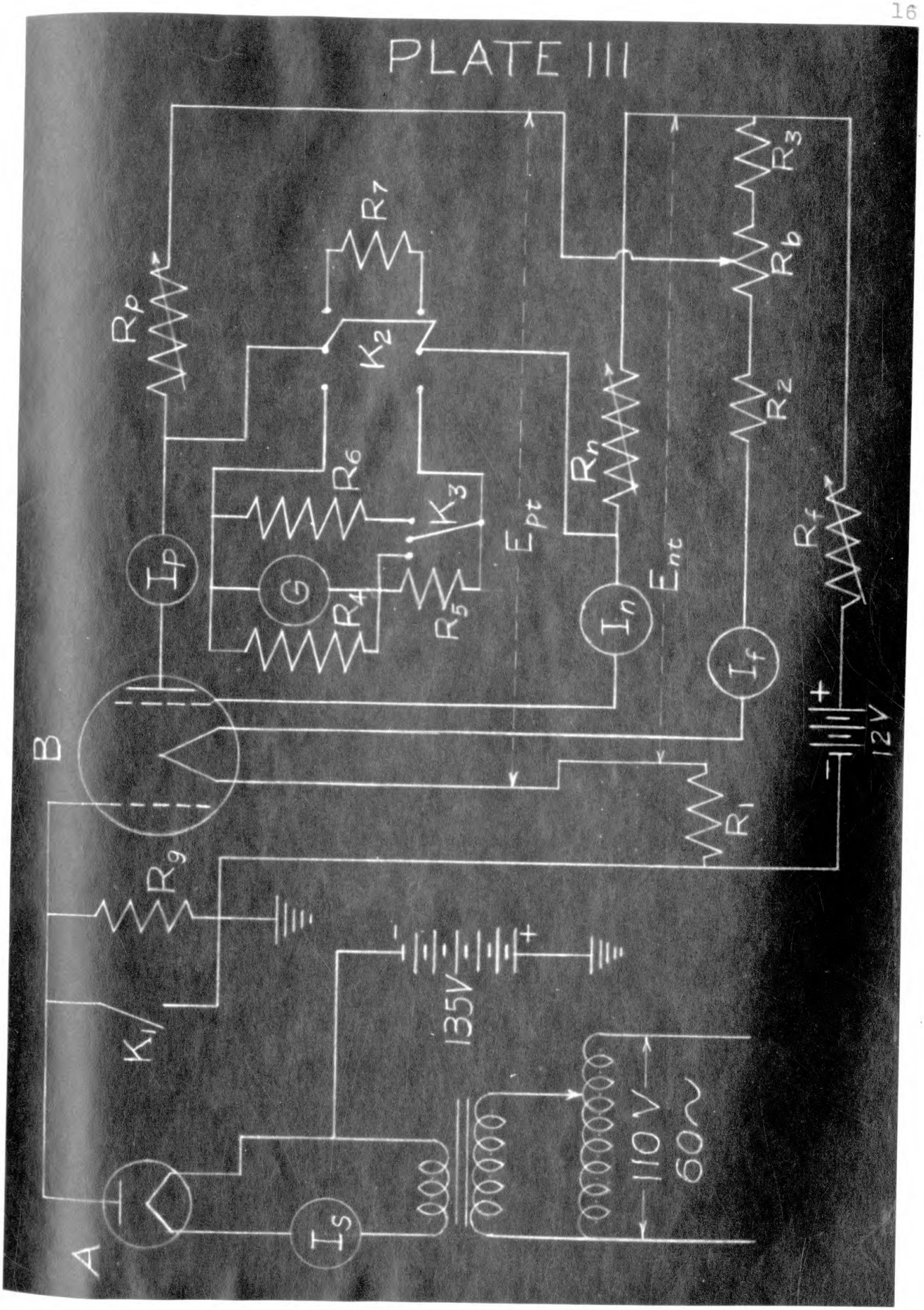
PLATE III
A
B
I_s
K_1
R_9
135V
110 V
60~
I_p
R_p
R_7
K_2
R_6
K_3
G
R_4
R_5
E_{pt}
R_n
I_n
E_{nt}
I_f
R_1
R_2
R_3
R_b
R_f
12V

in gaining stability, there should be the least possible loss in sensitivity. Penick (47) has compared a large number of balanced circuits and has concluded that the modified Barth circuit is the most generally adaptable. Because of the high sensitivity, it was necessary to shield all of the circuit connections from external fields.

The balancing procedure was as follows:

1. The resistance R_f was adjusted so that I_f = 270 milliamperes. A measurement of E_{nt} gave a value of 8.9 volts at this setting.
2. By changing the setting of R_b, the value of E_{pt} was altered. In a typical setting E_{pt} had a value of 6.35 volts.
3. With the galvanometer circuit open, R_p and R_n were adjusted until I_p and I_n took on approximately the values given in the technical data for the D-96475 tube. For stability, $E_{pt} - I_pR_p = E_{nt} - I_nR_n$.
4. When the galvanometer circuit was closed, an adjustment of R_p and R_n brought the galvanometer current to approximately zero.
5. To determine whether E_{pt} was too high or too low, I_f was varied slowly in small steps (by changing the setting of R_f) in order to judge the trend of the stability characteristic. The galvanometer deflection was plotted against I_f. If the galvanometer was connected to give a positive deflection when the plate was more positive than the space-charge grid, a positive slope indicated too low a value of E_{pt}, and conversely, a negative slope too high a value.

6. I_f was returned to normal and E_{pt} changed by a small amount in the proper direction by altering the setting of R_b. Then R_p and R_n were readjusted to bring the galvanometer current to zero and I_f varied again as in 5. This procedure was repeated as many times as necessary to obtain the desired precision of balance. When near the balance point, it was necessary to allow some time after each variation in I_f for the filament to reach temperature equilibrium.

Figure 2 shows a stability curve taken in the balancing procedure. The electrometer circuit was ready for use after obtaining such a curve near the balance point. Data for the electrometer circuit when this curve was taken were as follows:

E_{nt} = 8.9 volts
E_{pt} = 6.35 volts
I_n = 0.435 milliamperes
R_n = 9639 ohms
I_p = 86.5 microamperes
R_p = 19,000 ohms
Time interval between each variation in I_f = 5 minutes

Condition for balance, $E_{nt} - I_nR_n = E_{pt} - I_pR_p$

$8.9 - 4.19 = 6.35 - 1.64 = 4.71$ volts

The Ionization Gauge

An ionization gauge of the type described by Found and Dushman (26) was used to measure the extremely low pressures necessary in this experiment. The gauge used here was a

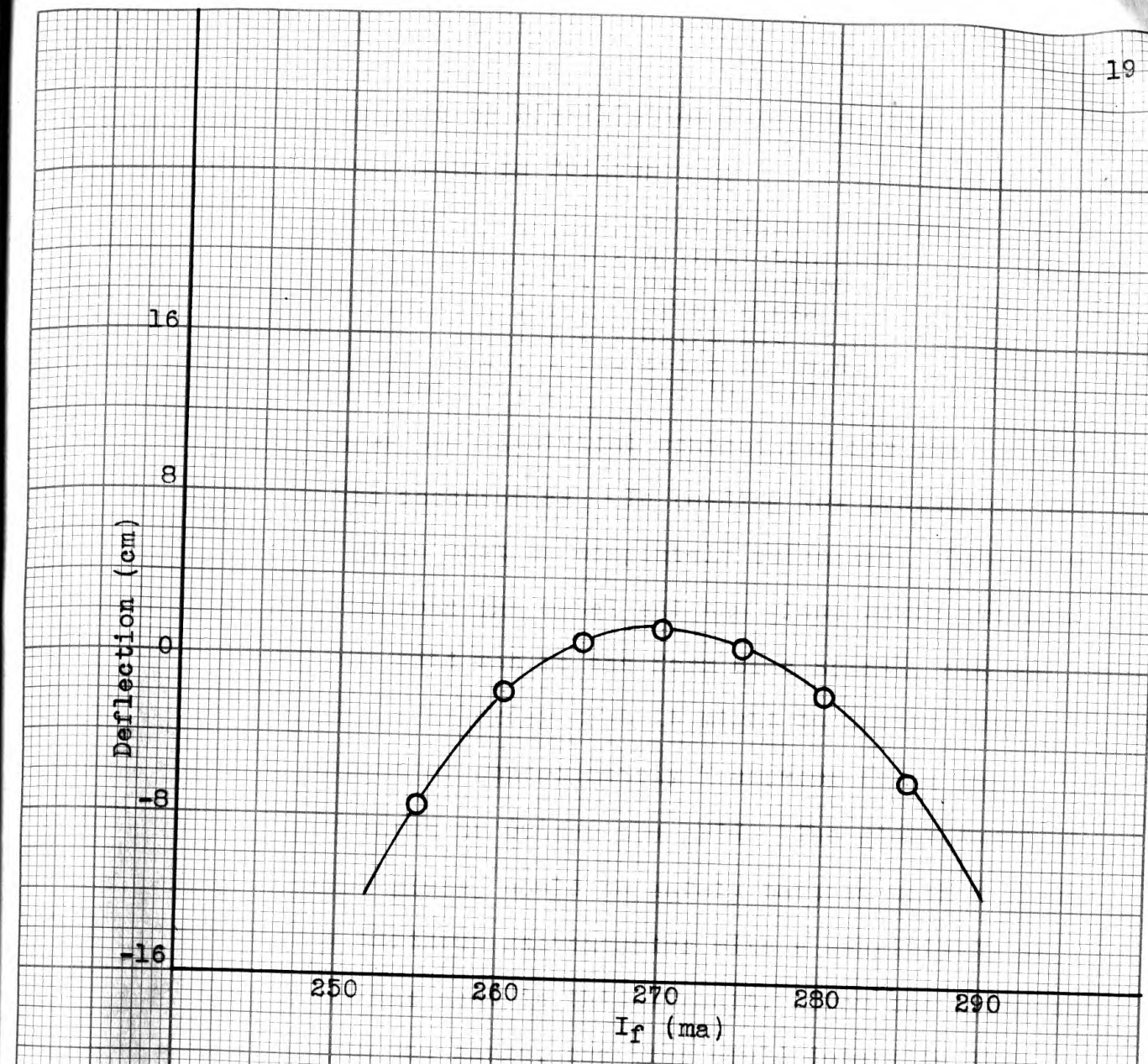

Fig. 2. Typical stability curve obtained in the balancing procedure.

Type VG-1 manufactured by Distillation Products, Inc. Physical data for this gauge were as follows:

Collector	thin film--platinum
Grid	spiral--tungsten
Filament	pure tungsten
Envelope	pyrex glass
Height	3-1/2 in.
Diameter	1-1/2 in. o.d.
Tubulation	5/8 in. i.d.

Plate IV shows the electrical connections for the ionization gauge and its accessories. In reading low pressures, the elements of the gauge must be completely outgassed. Otherwise, gas evolution from both the metal and the glass would produce poor results. The grid was in the form of a spiral, and two leads were available in order that it might be heated electrically. A current of approximately 7 amperes for a few minutes was sufficient to outgas the grid. The glass envelope, being made of hard glass, could be safely torched with a flame.

A Leeds and Northrup galvanometer with a sensitivity of 0.00045 μa per mm was used in this circuit. From the technical data supplied with the gauge, one then could determine the pressure in the system by the scale deflection of the galvanometer during a typical operation. Typical operation data were as follows:

Filament	3.5 volts, 5 amperes
Grid	+150.0 volts, 5 milliamperes
Collector	-25.0 volts, 1.5 microamperes
Pressure	10^{-5} mm of mercury

The equivalent pressures for various scale deflections could then be determined from the sensitivity of the galvanometer and the distance from the galvanometer to the scale. Equivalent

EXPLANATION OF PLATE IV

Circuit for ionization gauge, Type VG-1.

I_1 - Weston A.C. ammeter, range 0-10 amp.

I_2 - Weston A.C. ammeter, range 0-10 amp.

I_3 - Weston D.C. milliammeter, range 0-15 ma.

G - Leeds and Northrup galvanometer, sensitivity 0.00045 ua/mm, damping resistance 9200 ohms, period 6.25 sec, internal resistance 484 ohms.

M - Ionization manometer, Type VG-1.

K_1 - DPDT switch.

K_2 - SPST switch.

PLATE - IV

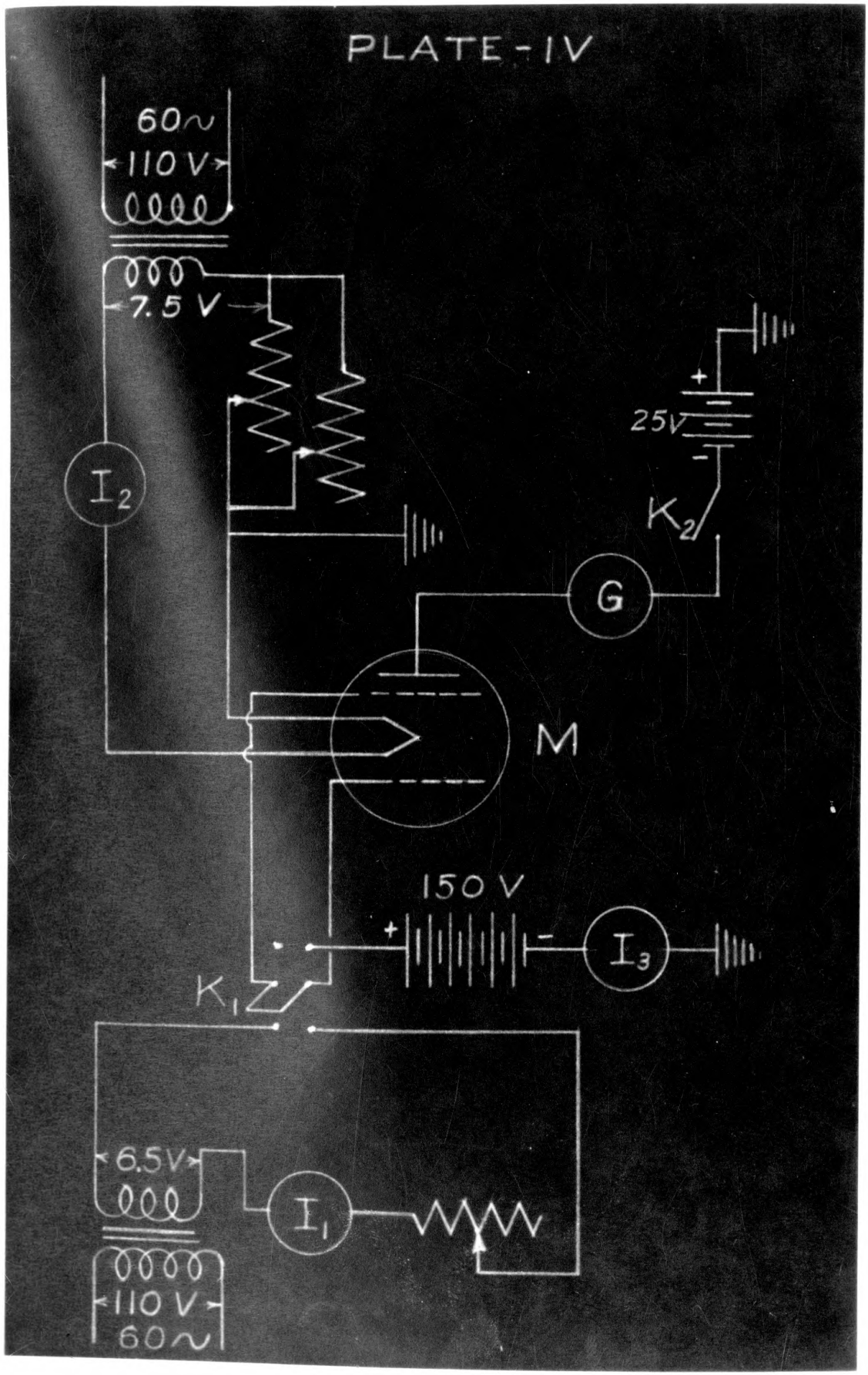

scale deflections and pressure were as follows:

Deflection	Pressure
400 cm	10^{-5} mm of Hg
40 cm	10^{-6}
4 cm	10^{-7}
4 mm	10^{-8}

Temperature Measurement

Temperatures were measured with a Leeds and Northrup optical pyrometer of the disappearing filament type. The pyrometer was focused on the nickel strip through the optically flat pyrex window.

Black body corrections for emissivity were made on the pyrometer readings according to the temperature scale of Wahlin and Wright (56). These temperature corrections are given in Table 2.

Table 2. Temperature scale for nickel (Wahlin and Wright, 56).

True temperature	Apparent temperature
1175 °K	1111.4 °K
1200	1133.3
1225	1155.8
1250	1178.0
1275	1200.1
1300	1222.2
1325	1244.3
1350	1266.3
1375	1288.5
1400	1310.3
1425	1332.6
1450	1354.6
1475	1376.9
1500	1399.6

Source and Intensity of Monochromatic Light

The source of ultraviolet light was a quartz mercury arc of the vertical type, Utility Model SC-5030 manufactured by Hanovia Chemical and Manufacturing Company. It was operated at a current of 2.5 amperes with 117 volts drop in potential across the arc. This resulted in quite intense illumination and reduced the maximum variation of light intensity to approximately three per cent.

Light from the arc was focused through an auxiliary quartz lens onto the entrance slit of the Bausch and Lomb quartz monochromator. The widths of the entrance and exit slits of the monochromator were 0.04 and 0.03 cm, respectively. To prevent stray light being reflected from the walls of the room to the specimen in the experimental tube, it was necessary to construct a large black box to enclose completely the mercury arc. Then only light that had passed through the quartz monochromator could fall on the nickel strip. The wave lengths used in this experiment were chosen from characteristic lines produced by a mercury arc. Plate V is a copy of Lord Rayleigh's (48) photograph of this spectrum which facilitated the choice of desirable lines.

The intensity of each line was measured by an Eppley bismuth-silver, eight-junction vacuum thermopile, mounted on the front of the monochromator. This thermopile had a resistance of 7.5 ohms and a sensitivity of 0.0396 microvolts per microwatt per square centimeter. The thermopile attachment was constructed

EXPLANATION OF PLATE V

Photograph of mercury spectrum (Lord Rayleigh, 48), showing principal lines available for production of photoelectrons.

PLATE V

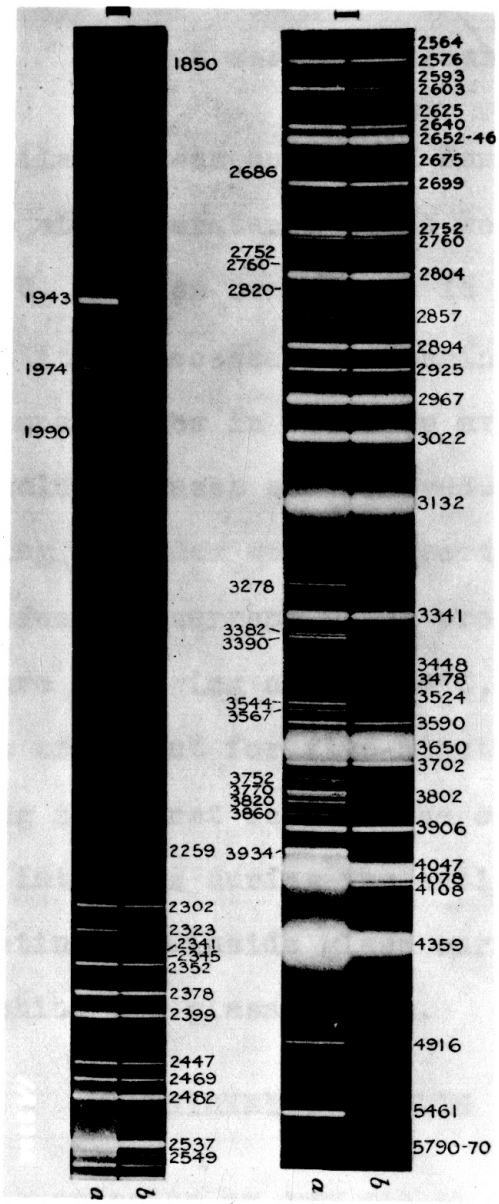
1850
1943
1974
1990
2259
2302
2323
2341
2345
2352
2378
2399
2447
2469
2482
2537
2549
2686
2752
2760
2820
3278
3382
3390
3544
3567
3752
3770
3820
3860
3934
2564
2576
2593
2603
2625
2640
2652-46
2675
2699
2752
2760
2804
2857
2894
2925
2967
3022
3132
3341
3448
3478
3524
3590
3650
3702
3802
3906
4047
4078
4108
4359
4916
5461
5790-70
a
b
a
b

so that it could be lowered over the exit slit as needed. The thermopile was connected to a Leeds and Northrup HS galvanometer having a sensitivity of 0.0015 μa per mm, a period of eight seconds, and a resistance of 15.6 ohms.

The Outgassing Process

The nickel filament was outgassed for a period of approximately 850 hours at temperatures which were gradually increased from 400 to 1200°C. It has been found in previous experiments of this type that it is necessary to begin the outgassing process at low temperatures in order to avoid excessive evaporation as the occluded gases are removed.

The collecting cylinder was outgassed by heating with a high frequency induction current which produced a rather non-uniform temperature averaging about 750°C. The cylinder was subjected to this treatment for five-minute intervals several times a day during the first days of the outgassing period.

At frequent intervals during the entire outgassing period, the gas contaminating the inside glass surfaces was partially liberated by torching the glass system.

EXPERIMENTAL RESULTS

Photoelectric emission on two nickel specimens caused by different wave lengths of ultraviolet radiation was taken at various stages in the outgassing process.

Table 3 gives data for partially outgassed nickel at 313°K, and these data are shown graphically in Figs. 3 and 4. In Fig. 3 the photocurrent per unit light intensity is plotted against wave length. Figure 4 is a Fowler plot of the experimental data where the ordinate is $\log_e I/T^2$ and the abscissa is $h\nu/kT$. Here I is the photocurrent per unit light intensity, T is the absolute temperature, h is Planck's constant, k is Boltzmann's constant, and ν is the frequency of the exciting radiation. The horizontal shift of the points in order to superimpose them upon Fowler's theoretical curve (see Fig. 1) enables one to determine the work function characteristic of the surface at 0°K. The work function for this curve is obtained as follows:

$$\text{horizontal shift} = h\nu_0/kT = 167.8$$

$$\phi = \frac{h\nu_0}{1.6\times10^{-12}} = \frac{167.8\ kT}{1.6\times10^{-12}} = 4.50 \text{ electron-volts}$$

Table 3. Experimental data for partially outgassed nickel (T = 313°K).

Wave length (A.u.)	Average photocurrent (cm)	Average light intensity (cm)	Photocurrent per unit light intensity	$\frac{h\nu}{kT}$	$\log_e \frac{I}{T^2}$
2378	4.6	1.8	2.56	192.5	-10.55240
2399	3.1	1.5	2.07	190.8	-10.76486
2482	2.75	2.9	0.95	184.4	-11.54370
2537	3.9	6.2	0.63	180.5	-11.95444
2649	1.7	7.7	0.22	172.8	-13.00643
2699	0.7	3.4	0.02	169.6	-15.40440

Typical data for carefully outgassed nickel are shown in Table 4 and plotted in Figs. 5 and 6. In Fig. 5, the asymptotic approach to the axis is more evident at the higher temperature than at the lower temperature. Data for these curves were taken

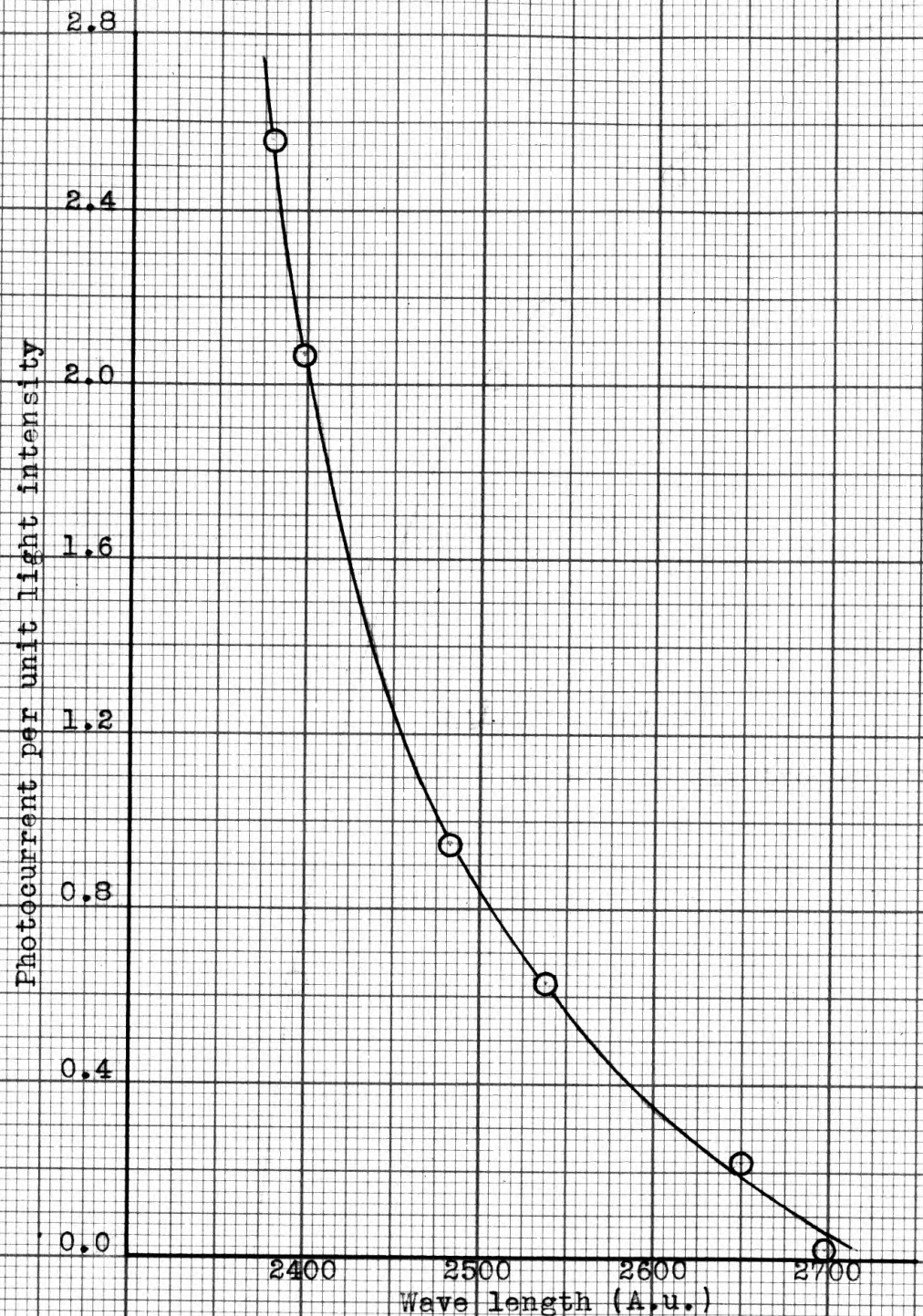

Fig. 3. Photoelectric sensitivity curve for partially outgassed nickel.

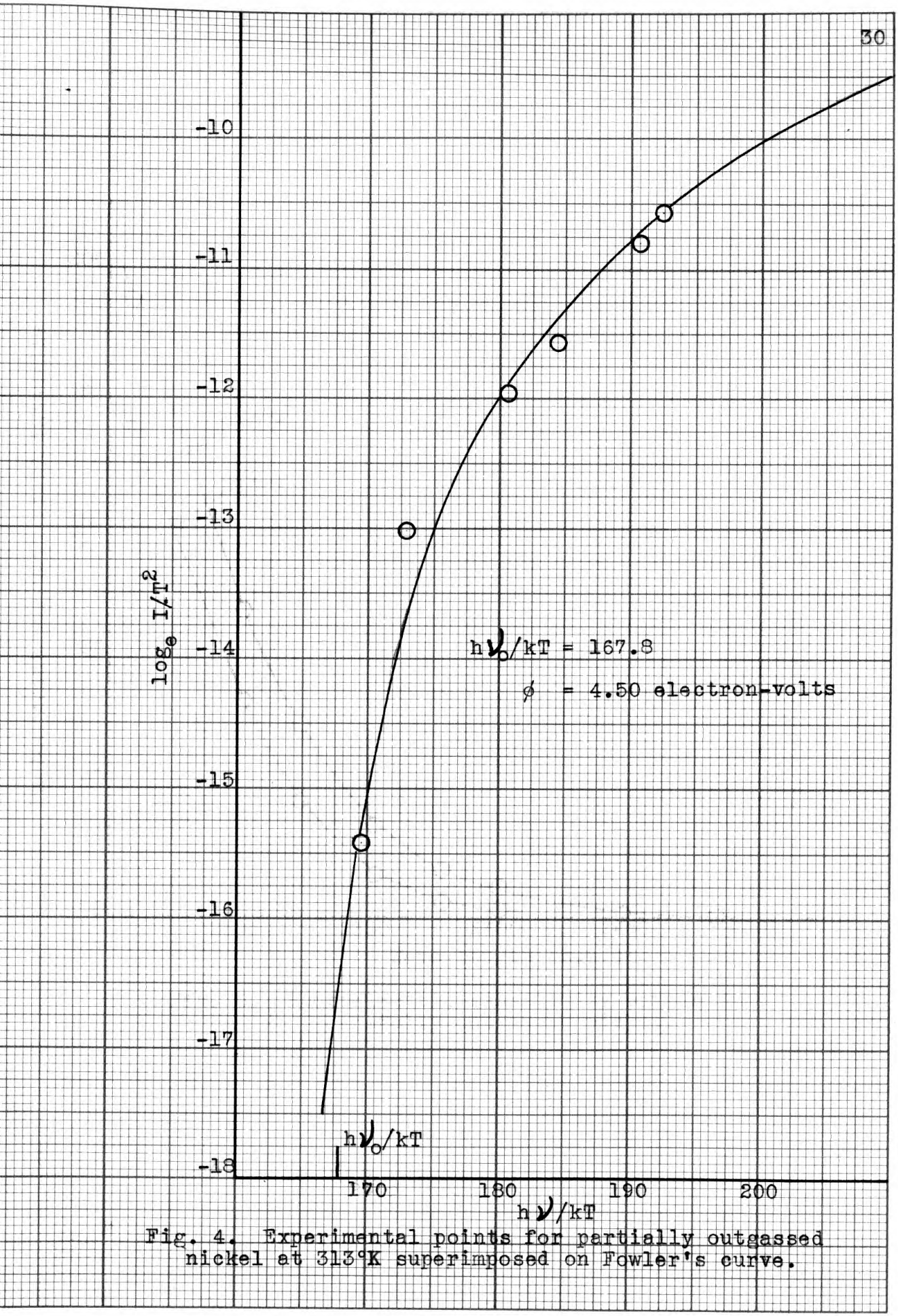

Fig. 4. Experimental points for partially outgassed nickel at 313°K superimposed on Fowler's curve.

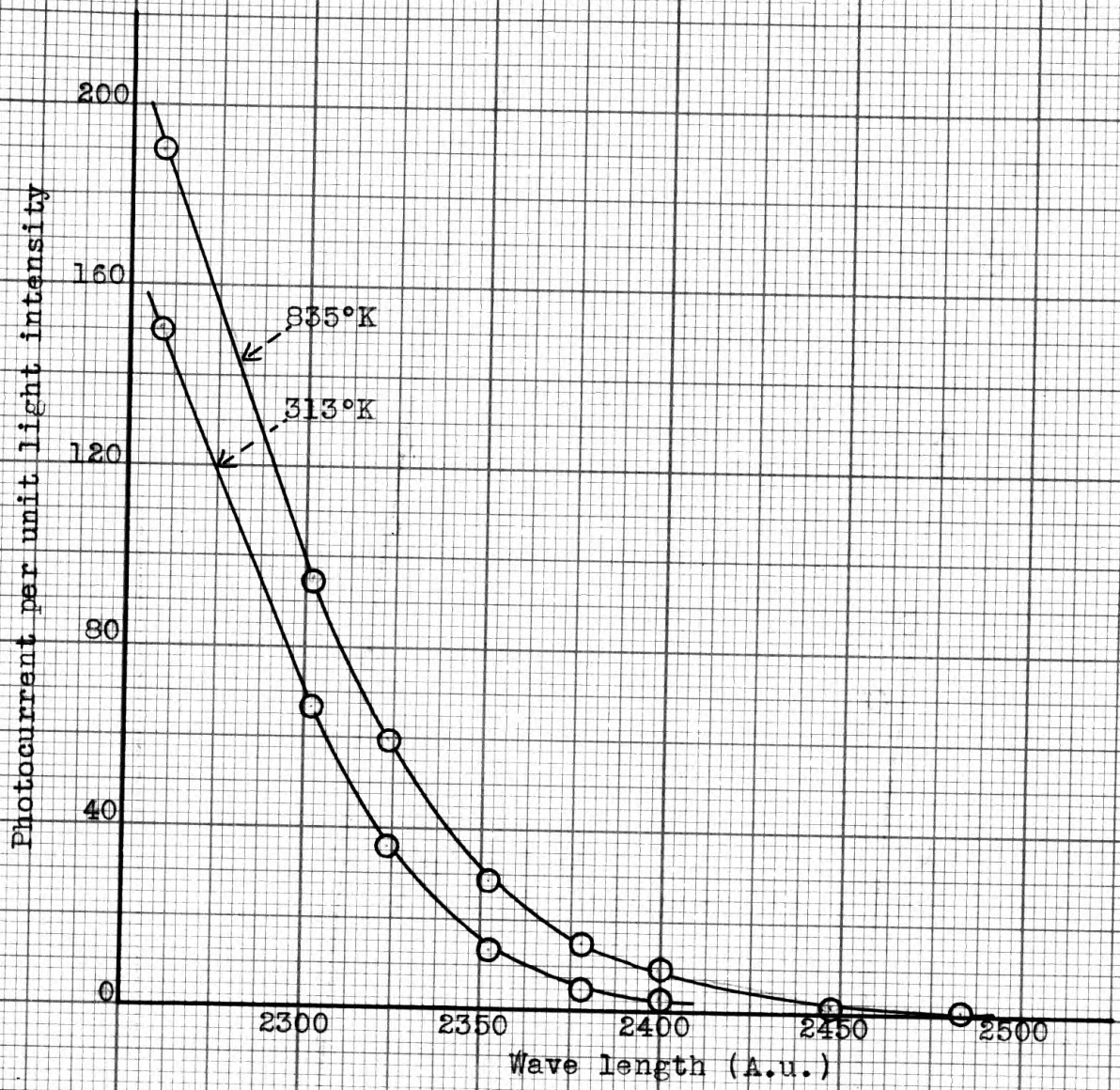

Fig. 5. Photoelectric sensitivity curves for carefully outgassed nickel.

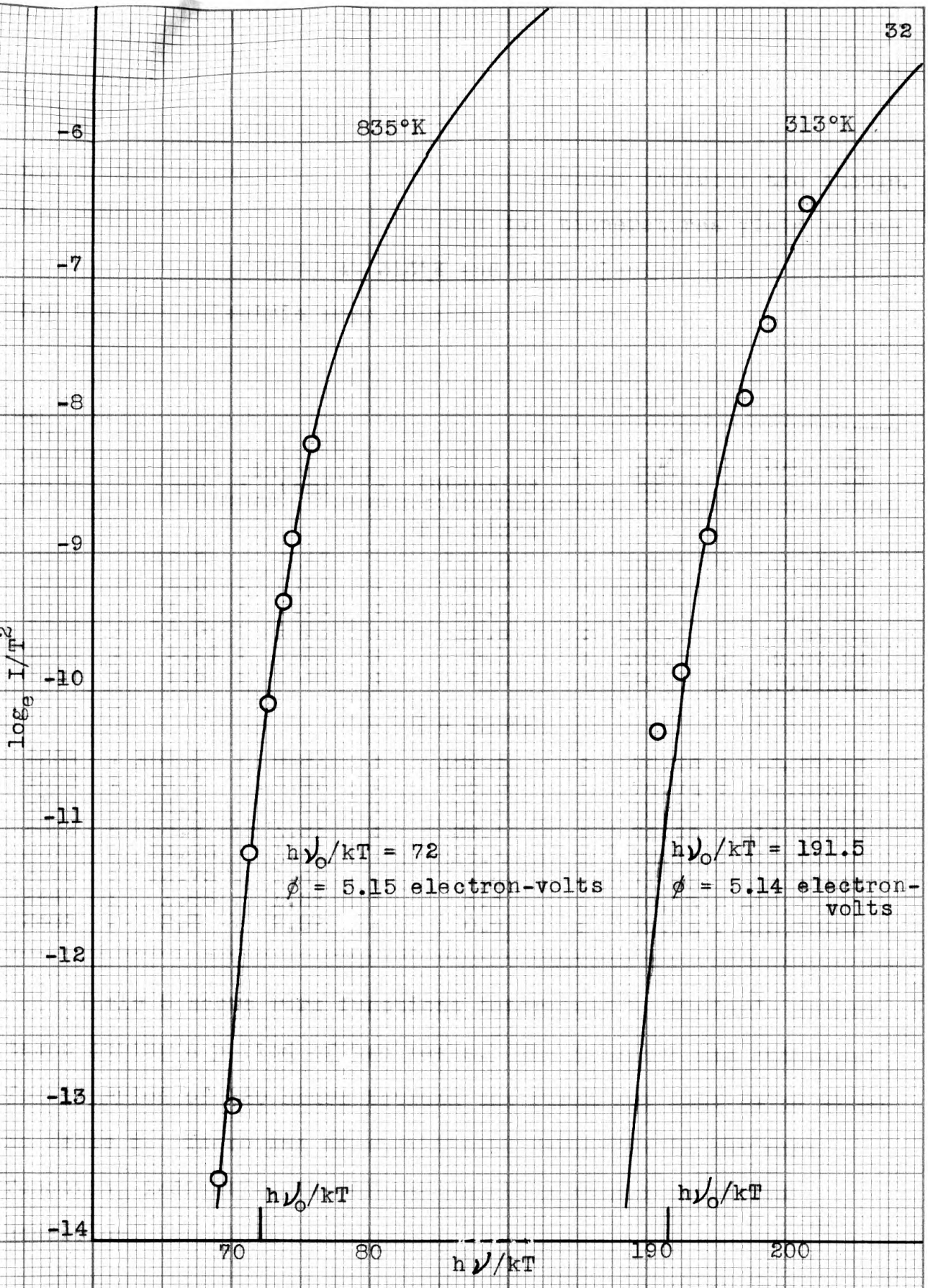

Fig. 6. Experimental points for carefully outgassed nickel at 313°K and 835°K superimposed on Fowler's theoretical curve.

simultaneously, and if there were a different work function at the higher temperature, a Fowler plot should indicate the change. The Fowler plots in Fig. 6 for the two temperatures yield values of 5.14 electron-volts at 313°K and 5.15 electron-volts at 835°K for the photoelectric work function of nickel.

Table 4. Experimental data for carefully outgassed nickel at low and high temperatures.

Wave length (A.u.)	Average photocurrent (cm)	Average light intensity (cm)	Photocurrent per unit light intensity	$\frac{h\nu}{kT}$	$\log_e \frac{I}{T^2}$
			T = 313°K		
2259	122.3	0.81	151.0	202.7	-6.47512
2302	64.2	0.96	66.9	198.9	-7.28921
2323	34.3	0.94	36.5	197.1	-7.89509
2352	16.5	1.21	13.6	194.6	-8.88234
2378	9.15	1.61	5.1	192.5	-9.87104
2399	4.6	1.40	3.3	190.8	-10.30152
			T = 835°K		
2259	153.3	0.81	189.3	75.96	-8.21153
2302	92.6	0.96	96.5	74.94	-8.88532
2323	56.3	0.94	59.9	73.87	-9.36219
2352	35.2	1.21	29.1	72.96	-10.08413
2378	24.85	1.61	15.4	72.16	-10.72050
2399	13.75	1.40	9.8	71.53	-11.17248
2447	1.85	1.26	1.5	70.13	-13.04939
2482	2.3	2.57	0.9	69.14	-13.55986

Table 5 shows work functions determined by Fowler's method taken during a period of two weeks. The filament was outgassed for a period of 220 hours between the first and last value shown in Table 5. There was no significant variation in the work function, indicating the nickel was in a stable outgassed condition.

Table 5. Values for work function of outgassed nickel determined by Fowler's method.

Date	Work function in electron-volts	Temperature in degrees Kelvin
June 26	5.12	313
July 3	5.14	313
July 5	5.13	835
July 6	5.14	313
	5.15	835
July 7	5.14	313
	5.19	1040
Average = 5.14 ± 0.03		

The value, 5.14 electron-volts, obtained for carefully outgassed nickel is not in agreement with the value (4.61 electron-volts) recently obtained thermionically by Wahlin (53). It is interesting to note that his value agrees approximately with that obtained in this work during the initial outgassing stage. Wahlin used a wire rather than a thin strip. It is generally recognized that increasing the thickness of a specimen greatly hampers the driving off of the occluded gases. It is believed the sample studied by Wahlin was never gas-free and consequently that he obtained a work function characteristic of a partially gas-filled nickel surface.

The work function obtained here is in the range of that (5.01 electron-volts) reported by Glasoe (29) who studied the photoelectric emission of nickel at room temperature only. Glasoe's experimental arrangement was superior to that of Wahlin and would be expected to yield results more nearly characteristic of a gas-free surface. This value is also in

close agreement with the thermionic work function (5.03 ± 0.05 electron-volts) obtained by Fox and Bowie (27).

No reliable thermionic data were obtained. The first nickel sample burned out after approximately 200 hours of outgassing, and no thermionic data had been taken on it. The second sample was outgassed for a period of approximately 850 hours, burning out before data for a complete thermionic curve had been obtained. These data, although incomplete, indicated a thermionic work function in the neighborhood of the photoelectric work function.

An unexpected effect was observed when the photocurrent was obtained as a function of the temperature, the wave length of the exciting radiation remaining constant. Figure 7 shows curves for three wave lengths as the heating current (temperature) through the nickel was increased and decreased. These curves show a marked change in the photoelectric sensitivity at a temperature which is in the neighborhood of the known α-β transition of nickel. Since data obtained above and below this temperature indicate no change in work function, it is difficult to explain these curves. The only plausible explanation is to be found in the assumption that either the quantum efficiency is a function of the temperature or the optical reflection coefficient is a function of temperature. In either case, there is no apparent reason for the required function.

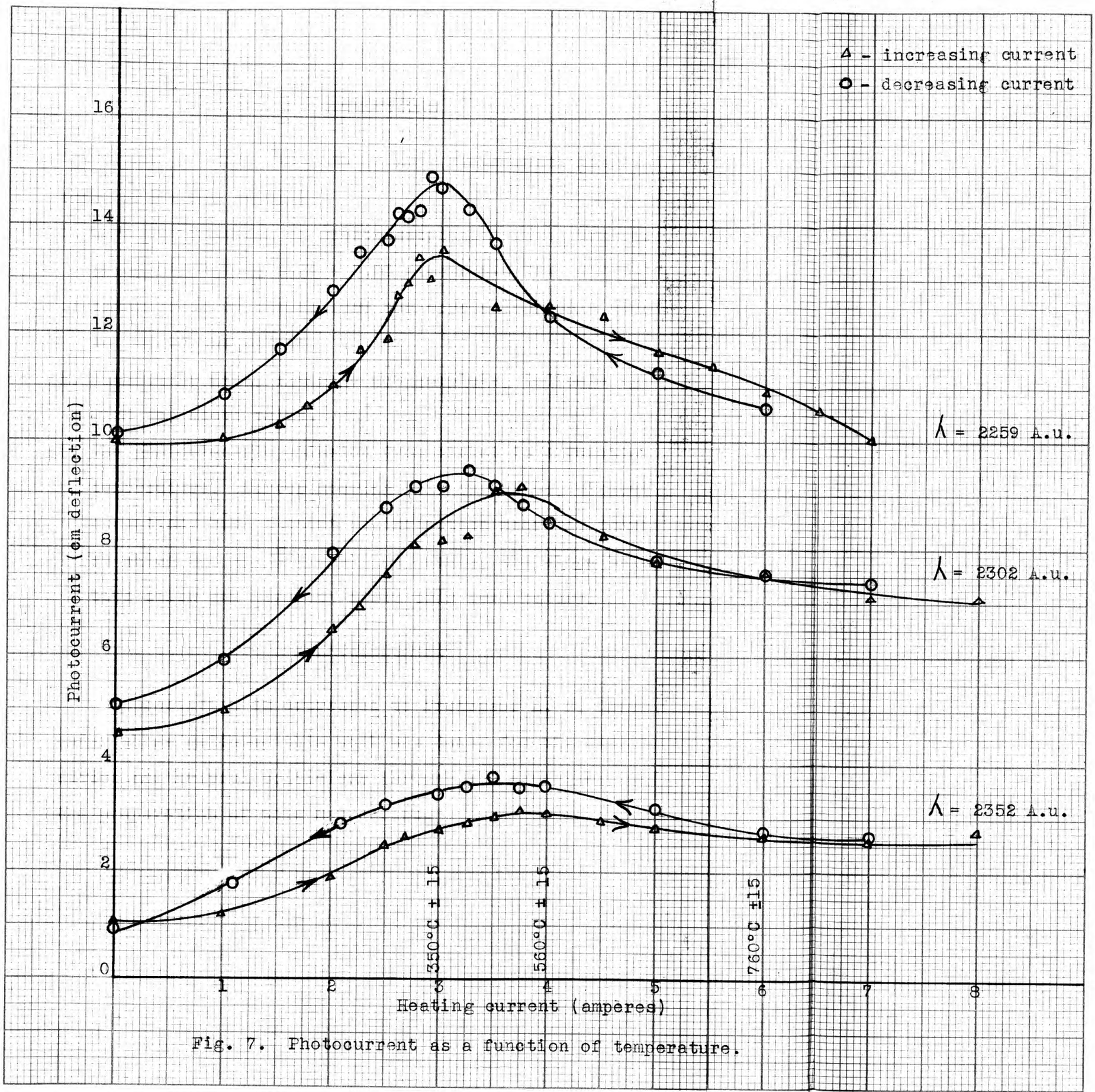

Fig. 7. Photocurrent as a function of temperature.

CONCLUSIONS

From the data obtained in this experiment, the following conclusions are reached:

1. The work function of spectroscopically pure, carefully outgassed nickel is 5.14 ± 0.03 electron-volts, and it is independent of temperature and crystallographic transformation if one exists.
2. Thermionic data, although not complete, indicate agreement with the above value.
3. The photoelectric emission from nickel is a function of temperature. Curves showing this variation, without exception, have a point of inflection near the temperature at which the α-β transition occurs, the slope being positive below and negative above this temperature.

ACKNOWLEDGMENT

Appreciation is expressed to Professor A. B. Cardwell, under whose guidance this work was done, for his excellent advice and helpful criticisms through the experiment and the preparation of this manuscript.

LITERATURE CITED

(1) Barth, G.
Über ein neuartiges Rohrengalvanometer. Zeits. f. Physik, 87: 399-408. Jan. 1934.

(2) Bomke, H.
Photoelectric properties of cadmium, especially as affected by gases. Ann. d. Physik, 10: 579-615. July, 1931.

(3) Bredig, G., and Allolio, R.
Röntgenuntersuchungen an katalytisch wirkenden Metallen. Zeits. phys. Chem. 126: 41-71. March, 1927.

(4) Bredig, G., and Schwarz von Bergkampf, E.
Über Hexagonales Nickel. Z. physik. Chem., Bodenstein-Festband, pp. 172-176. 1931.

(5) Cardwell, A. B.
Effects of a crystallographic transformation on the photoelectric and thermionic emission from cobalt. Nat. Acad. Sci., Proc. 15: 544-551. July, 1929.

(6) _____
Photoelectric and thermionic emission from cobalt. Phys. Rev. 38: 2033-2040. Dec. 1931.

(7) _____
The photoelectric and thermionic properties of iron. Nat. Acad. Sci., Proc. 14: 439-445. June, 1928.

(8) _____
The photoelectric properties of tantalum. Phys. Rev. 38: 2041-2048. Dec. 1931.

(9) _____
The thermionic properties of tantalum. Phys. Rev. 47: 628-630. April, 1935.

(10) Cashman, R. J., and Bassoe, E.
Surface and volume photoelectric emission from barium. Phys. Rev. 55: 63-69. Jan. 1939.

(11) Cashman, R. J., and Huxford, W. S.
Photoelectric sensitivity of magnesium. Phys. Rev. 43: 811-818. May, 1933.

(12) _____
Photoelectric properties of pure and gas-contaminated magnesium. Phys. Rev. 48: 734-741. Nov. 1935.

(13) Compton, A. H., and Compton, K. T.
A sensitive modification of the quadrant electrometer: its theory and use. Phys. Rev. 14: 85-98. Aug. 1919.

(14) DeVoe, C. F.
Photoelectric properties of zinc. Phys. Rev. 50: 481-485. Sept. 1936.

(15) Dillon, J. H.
Photoelectric properties of zinc single crystals. Phys. Rev. 38: 408-415. Aug. 1931.

(16) Dixon, E. H.
Some photoelectric and thermionic properties of rhodium. Phys. Rev. 37: 60-69. Jan. 1931.

(17) DuBridge, L. A.
Variations in the photoelectric sensitivity of platinum. Nat. Acad. Sci., Proc. 12: 162-168. March, 1926.

(18) _____
The photoelectric and thermionic work functions of outgassed platinum. Phys. Rev. 31: 236-243. Feb. 1928.

(19) DuBridge, L. A., and Roehr, W. W.
Thermionic and photoelectric work functions of molybdenum. Phys. Rev. 42: 52-57. Oct. 1932.

(20) _____
Photoelectric and thermionic properties of palladium. Phys. Rev. 39: 99-118. Jan. 1932.

(21) Dunn, H. K.
Changes in the photo-electric threshold of mercury. Phys. Rev. 29: 693-700. May, 1927.

(22) Einstein, A.
Generation and transformation of light. Ann. d. Physik, 17: 132-148. June, 1905.

(23) _____
Light generation and absorption. Ann. d. Physik, 20: 199-206. May, 1906.

(24) Engelmann, A.
Photoelectric threshold of rhenium. Ann. d. Physik, 17: 185-208. May, 1933.

(25) Ewert, M.
The specific heats and the allotropism of nickel between 0° and 1000°C. Roy. Acad. Amsterdam, Proc. 39: 833-838. 1936.

(26) Found, C. G., and Dushman, S.
Studies with ionization gauge. Phys. Rev. 23: 734-743. June, 1924.

(27) Fox, G. W., and Bowie, R. M.
A new method for determining the thermionic work functions of metals and its application to nickel. Phys. Rev. 44: 345-348. Sept. 1933.

(28) Fowler, R. H.
The analysis of photoelectric sensitivity curves for clean metals at various temperatures. Phys. Rev. 38: 45-56. July, 1931.

(29) Glasoe, G. N.
Contact potential difference between iron and nickel and their photoelectric work functions. Phys. Rev. 38: 1490-1496. Oct. 1931.

(30) Goetz, A.
The photoelectric effect of molten tin and two of its allotropic modifications. Phys. Rev. 33: 373-385. March, 1929.

(31) Hales, W. B.
Critical photoelectric potential of clean mercury and the influence of gases and of the circulation of the mercury upon it. Phys. Rev. 32: 950-960. Dec. 1928.

(32) Hallwachs, W.
Ueber den Einfluss des Lichtes auf electrostatisch geladene Körper. Ann. Phys. Chem. 33: 301-312. 1888.

(33) Hertz, H.
Ueber einen Einfluss des ultravioletten Lichten auf die electrische Entladung. Ann. Phys. Chem. 31: 983-1000. 1887.

(34) Hole, W. L., and Wright, R. W.
Emissive and thermionic characteristics of uranium. Phys. Rev. 56: 785-787. Oct. 1939.

(35) Hughes, A. L.
On the emission velocities of photoelectrons. Phil. Trans. Roy. Soc. 212: 205-226. 1912.

(36) Jamison, N. C., and Cashman, R. J.
Photoelectric properties of barium and calcium. Phys. Rev. 50: 624-631. Oct. 1936.

(37) Jupnik, H.
Photo-electric properties of bismuth. Phys. Rev. 60: 884-889. Dec. 1941.

(38) Kazda, C. B.
The photo-electric threshold for mercury. Phys. Rev. 26: 643-654. Nov. 1925.

(39) Lenard, P.
Production of kathode rays by ultra-violet light. Ann. d. Physik, 2: 359-379. June, 1900.

(40) _____
Light electric effect. Ann. d. Physik, 8: 149-198. April, 1902.

(41) Martin, M. J.
The photoelectric and thermionic properties of molybdenum. Phys. Rev. 33: 991-997. June, 1929.

(42) Masumoto, H.
On a new transformation of cobalt and equilibrium diagrams of nickel-cobalt and iron-cobalt. Sci. Rep. Tohoku Univ. 15: 449-475. 1926.

(43) Mazza, L., and Nasini, A. G.
The crystal structure of nickel. Phil. Mag. 7: 301-311. Feb. 1929.

(44) Merica, P. D.
Physical and mechanical properties of nickel. Amer. Soc. for Steel Treating, Trans. 15: 1054-1059. 1929.

(45) Millikan, R. A.
A direct photoelectric determination of Planck's "h". Phys. Rev. 7: 355-388. March, 1916.

(46) Morris, L. W.
Certain photoelectric properties of gold. Phys. Rev. 37: 1263-1268. May, 1931.

(47) Penick, D. B.
Direct-current amplifier circuits for use with the electrometer tube. Rev. Sci. Inst. 6: 115-120. April, 1935.

(48) Rayleigh, Lord
Luminous vapour from the mercury arc and the progressive changes in its spectrum. Roy. Soc. London, Proc. 108: 262-279. 1925.

(49) Reiman, A. L.
Thermionic emission from carbon. Phys. Soc., Proc. 50: 496-500. July, 1938.

(50) Richardson, O. W., and Compton, K. T.
The photoelectric effect. Phil. Mag. 24: 575-594. Oct. 1912.

(51) Sommerfeld, A.
Zur Elektronentheorie der Metalle auf Grund der Fermischen Statistik. Zeits. f. Physik, 47: 1-60. Feb. 1928.

(52) Thompson, G. P.
Diffraction of cathode rays. Roy. Soc. London, Proc. 125A: 352-370. Sept. 1929.

(53) Wahlin, H. B.
Thermionic properties of the iron group. Phys. Rev. 61: 509-512. April, 1942.

(54) Wahlin, H. B., and Reynolds, J. A.
Positive and negative thermionic emission from molybdenum. Phys. Rev. 48: 751-754. Nov. 1935.

(55) Wahlin, H. B., and Sordahl, L. O.
Positive and negative thermionic emission from columbium. Phys. Rev. 45: 886-889. June, 1934.

(56) Wahlin, H. B., and Wright, R.
Emissivities and temperature scales of the iron group. J. App. Phys. 13: 40-42. Jan. 1942.

(57) Warner, A. H.
A comparison of the thermionic and photoelectric work functions for clean tungsten. Nat. Acad. Sci., Proc. 13: 56-60. Feb. 1927.

(58) _____
Variation of the photoelectric effect with temperature and determination of the long wave-length limit of tungsten. Phys. Rev. 33: 815-818. May, 1929.

(59) _____
The determination of the photoelectric threshold for tungsten by Fowler's method. Phys. Rev. 38: 1871-1875. Nov. 1931.

(60) Whitney, L. V.
Thermionic emission of platinum. Phys. Rev. 50: 1154-1157. Dec. 1936.

(61) Winch, R. P.
The photoelectric properties of silver. Phys. Rev. 37: 1269-1275. May, 1931.

(62) Winch, R. P., and Farnsworth, H. E.
Photoelectric work functions of (100) and (111) faces of silver single crystals and their contact potential difference. Phys. Rev. 58: 812-819. Nov. 1940.

(63) Wright, R. W.
Positive and negative thermionic emission from molybdenum. Phys. Rev. 60: 465-467. Sept. 1941.